# Fabrication and superconductivity of Na$_x$TaS$_2$ crystals

L. Fang,[1,2] Y. Wang,[1] P. Y. Zou,[1] L. Tang,[1] Z. Xu,[2] H. Chen,[1] C. Dong,[1] L. Shan,[1] and H. H. Wen[1,*]

[1]*National Laboratory for Superconductivity, Institute of Physics, Chinese Academy of Sciences, P.O. Box 603,*
*Beijing 100080, People's Republic of China*

[2]*Department of Material Science and Engineering, Tongji University, Shanghai 200092, People's Republic of China*

In this paper we report the growth and superconductivity of Na$_x$TaS$_2$ crystals. The structural data deduced from x-ray diffraction pattern shows that the sample has the same structure as 2H-TaS$_2$. A series of crystals with different superconducting transition temperatures ($T_c$) ranging from 2.5 K to 4.4 K were obtained. It is found that the $T_c$ rises with the increase of Na content determined by energy-dispersive x-ray microanalysis(EDX) of scanning electron microscope (SEM) on these crystals. Compared with the resistivity curve of un-intercalated sample 2H-TaS$_2$ ($T_c$=0.8 K, $T_{CDW} \approx 70$ K), no signal of charge density wave (CDW) was observed in samples Na$_{0.1}$TaS$_2$ and Na$_{0.05}$TaS$_2$. However, in some samples with lower $T_c$, the CDW appears again at about 65 K. Comparison between the anisotropic resistivity indicates that the anisotropy becomes smaller in samples with more Na intercalation (albeit a weak semiconducting behavior along *c*-axis) and thus higher $T_c$. It is thus concluded that there is a competition between the superconductivity and the CDW. With the increase of sodium content, the rise of $T_c$ in Na$_x$TaS$_2$ is caused mainly by the suppression to the CDW in 2H-TaS$_2$, and the conventional rigid band model for layered dichalcogenide may be inadequate to explain the changes induced by the slight intercalation of sodium in 2H-TaS$_2$.

PACS number(s): 74.25.Fy, 81.10.Fq, 74.25.Ha, 74.70.Dd

## I. INTRODUCTION

Layered transition-metal dichalcogenides (TMDC's) of the type $MX_2$ ($M$ is the transition metal, $X$=S, Se, Te) have been extensively studied for their rich electronic properties due to low dimensionality. Each layer of TMDC's consists of a hexagonal transition metal sheet sandwiched by two similar chalcogen sheets, the interaction between the $MX_2$ layers is weak and van der Waals-like. Charge density wave (CDW) and superconductivity (SC) coexist in this kind of materials. The electron-phonon coupling and its relationship with the CDW are investigated by angle resolved photoemission in 2H-TaSe$_2$ and 2H-NbSe$_2$ systems.[1] It is found that the CDW transition temperature decreases and meanwhile the superconducting critical temperature ($T_c$) increases from TaSe$_2$ through TaS$_2$ and NbSe$_2$ to NbS$_2$, which indicates that these two orders (CDW and superconductivity) compete with each other.[2,3]

Intercalation of atoms and molecules into the weak coupled region between the $MX_2$ layers leads to significant modification of properties, which is another highlight to study TMDC's. A variety of atoms and molecules were reported to be intercalated into the interlayer regions between the $MX_2$ layers, and the resulting compounds are superconducting.[4] Furthermore, different superconducting transition temperatures $T_c$ were found depending on the intercalated ions,[5,6] and the $T_c$ increased when the intercalated TMDC's were further hydrated.[7] The change of properties induced by intercalation may be explained in terms of charge transfer from the intercalated atoms or molecules to the host $MX_2$ layers, the band structure is unaltered upon intercalation, and density of states (DOS) at Fermi surface (FS) changes to reflect the transfer of charges from the intercalated atoms or molecules. This picture is called as the rigid-band model (RBM). The validity of this model is supported by some photoemission experiments and calculations for various intercalates of $MX_2$.[8–11]

In recent years, however, some experiments and calculations revealed that the change of properties of the intercalated $MX_2$ cannot be understood based on the rigid-band model. The electrical measurement of TaS$_2$(pyridine)$_{1/2}$ showed that there was no signal of CDW in the resistivity curve, which was attributed to the suppression of a structural instability by intercalation.[12] Angle-resolved photoemission was used to study the electronic band structures before and after the alkaline metal Cs and Na were intercalated into the 2H-TaSe$_2$ and VSe$_2$,[13–15] and it was found that the changes induced by intercalation was more extensive than that expected by the rigid-band model. The experiment of Na intercalation into 1T-TaS$_2$ also revealed that the properties of the CDW phases and the phase transitions are not only influenced by the shift of the Fermi-level in the Ta 5$d$ band, but also by the superstructure of the doped Na in the interlayer region.[16]

Therefore, it remains controversial whether it is possible to use the rigid-band model to explain the changes induced by the intercalation in TMDC's. In order to unravel this puzzle, more efforts are desired. In the family of TMDC's, the sample TaS$_2$ may be one of the model systems to tackle this problem. Two basic structures of TaS$_2$ were found and defined by the different orientation of stacking chalcogen sheets, one is 1T-TaS$_2$ with Ta in octahedral coordination with S atoms, another is 2H-TaS$_2$ with Ta in trigonal-prismatic coordination with S atoms.[17,18] The system 1T-TaS$_2$ shows four CDW phase transitions accompanied by changes in lattice parameters and resistivity when temperature decreases, the CDW formation could be explained by the Fermi surface nesting.[16,17,19] However, the system 2H

-$TaS_2$ is known for the existence of CDW order below 70 K and a superconducting transition at 0.8 K.[17,19] When sodium ions are intercalated into $2H$-$TaS_2$, $T_c$ increases. Polycrystalline samples of $Na_{0.33}TaS_2$ were made and reported to be superconductors below 4.7 K ($T_c^{oneset}$),[5,6] and the $T_c$ was increased to 5.5 K when the samples were hydrated.[7] In this paper, we report the growth of a series of crystals of $Na_xTaS_2$ (2H) with different superconducting transition temperatures. Measurements of x-ray diffraction and superconducting transition revealed good quality of these crystals.

## II. EXPERIMENT

Most layered compounds are known to intercalate atoms or molecules into the interlayer regions. A traditional way for fabricating intercalated layered dichalcogend compounds consists of two steps, the first step is to prepare polycrystalline compound or single crystal of $MX_2$ by chemical reaction or iodine-transport reaction.[7,20] Secondly, the intercalation is carried out by chemical treatments, the samples are dipped into concentrated solutions containing the intercalated atoms,[7,16,20] or exposed to metal vapors in a closed ampoule.[16] A new method suited for preparing samples for the studies of surface science was also reported, the intercalated compounds were prepared by *in situ* evaporation of metal atoms to the (0 0 0 1) cleaved surface of the TMDC's crystals. This process should be realized under the condition of ultra high vacuum (UHV).[14,21]

In this paper, we report the growth of crystals of $Na_xTaS_2$ directly with the chemical reaction. The starting materials are NaCl, Ta powder and sulfur powder with purity higher than 99.9%. The nominal mole ratio of NaCl, Ta, and S were 0.15, 1, and 2, respectively. They were mixed and thoroughly ground, then pressed into pellet, finally the pellet was sealed in an evacuated quartz tube. The tube was heated slowly up to 920 °C and sintered for 48 h then slowly cooled down to 700 °C with a cooling rate of $1-2$ °C/h. Finally the quartz tube was cooled down with furnace by shutting off the power. It is found that two kinds of crystals were obtained. A large number of black thin platelets grew on the inner side of the quartz tube. The surfaces of these platelets were rather wrinkled, but the subsequent AC diamagnetism measurement showed that these crystals had weak diamagnetic signal and broad transition. Another type of crystals were also black thin platelets which grew vertically on the surface of the pellet. The surface of the second kind of crystals was shiny and mirrorlike, but the number of them is quite limited. Subsequent x-ray diffraction pattern and AC diamagnetic measurement showed that this kind of crystal has the typical structure of $2H$-$TaS_2$ single crystal and sharp superconducting transition is observed on them. It is found that the size and the superconducting transition temperature of the second type of crystals are related to the cooling rate.

Figure 1 shows an enlarged view of one piece of $Na_{0.1}TaS_2$ crystals. The crystal is shiny and thin plateletlike with a clean and smooth surface. The dimension of the crystal is about $1.7 \times 1$ mm$^2$ and the thickness is about 0.1 mm. Figure 2 shows an enlarged view of the $Na_{0.1}TaS_2$ crystal at a corner. It is clear that the sample has a layered structure.
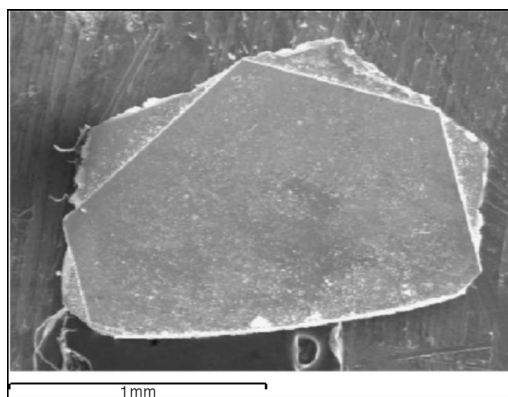


FIG. 1. An enlarged view of the $Na_{0.1}TaS_2$ crystal. The intercalated sodium content is determined by energy dispersive x-ray microanalysis (EDX) of SEM.

The x-ray diffraction pattern was performed at room temperature employing a M18AHF x-ray diffractometer (MAC Science). Crystallographic orientation and index are determined by Power-X, a programm for processing x-ray diffraction data.[22] The magnetic and transport measurements were carried out with an Oxford multiparameter measurement system (Maglab-Exa-12). The in-plane resistivity was determined by using standard four point measurement. The off-plane resistivity was measured by putting two separate pads of silver paste (one larger one for current and smaller one for voltage) on both sides of the sample. Since the in-plane resistivity is much smaller than the off-plane one, the whole area of the sample plane was taken as the cross-section area of the current flowing along $c$-aixs in determining $\rho_c$. The microscopic and concentration analysis is achieved with energy dispersive x-ray microanalysis (EDX) of a scanning electron microscope (Oxford).

## III. RESULTS AND DISCUSSION

### A. Structure and x-ray diffraction

Figure 3 presents the x-ray diffraction pattern at room temperature for one $Na_xTaS_2$ crystal. The XRD pattern is
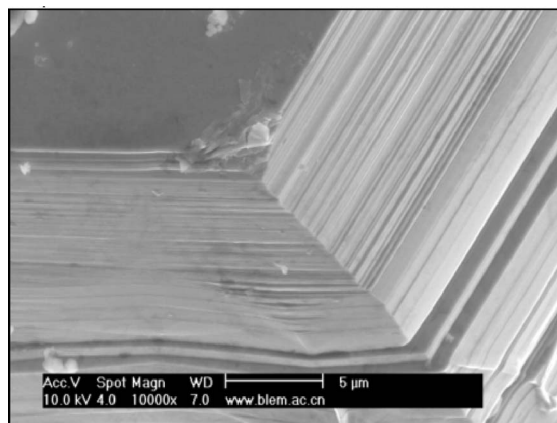


FIG. 2. An enlarged view of the $Na_{0.1}TaS_2$ crystal at a corner. It is obvious that the samples have a layered structure.
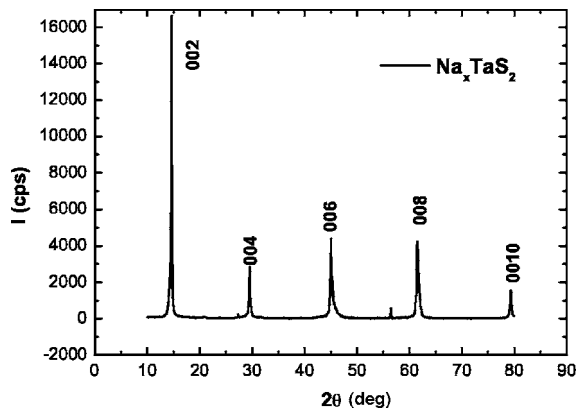
FIG. 3. X-ray diffraction pattern of a $Na_xTaS_2$ crystal. The $c$-axis lattice constant determined here is about $c=12.082$ Å which is quite close to that of $2H$-$TaS_2$. With increasing the Na content no obvious change of the $c$-axis constant has been observed in our samples.

indexed on the basis of hexagonal with $c=12.082$ Å, the value is quite close to the reported value $c=12.070$ Å,[23] and $c=12.097$ Å (Ref. 18) of $2H$-$TaS_2$. Further comparison with the value of $Na_{0.8}TaS_2$ ($c=14.36$ Å) indicates that only little content of sodium ions are intercalated into the interlayer regions of $2H$-$TaS_2$ in our present samples. The space group is $P\bar{6}m2$, which is the subgroup of $2H$-$TaS_2$ ($P6_3/mmc$). For more Na intercalated samples, the main peaks remain unshifted and sharp, no obvious change of the $c$-axis constant has been observed, but some commensurate modulation peaks around each main peak along the $c$-axis appear. Detailed analysis about these modulations will be presented in a forthcoming paper. Although the diffraction pattern is quite clean and the full-width at the half maximum (FWHM) of the diffraction peak is narrow, we cannot, however, rule out the possibility of some kind of stacking fault which often appear in the intercalated crystals. However we would argue that the stacking fault could be weak in our present case since only very little sodium are intercalated into the structure. Furthermore it remains unknown whether the intercalated sodium atoms are in a disordered state or organize into an ordered lattice.
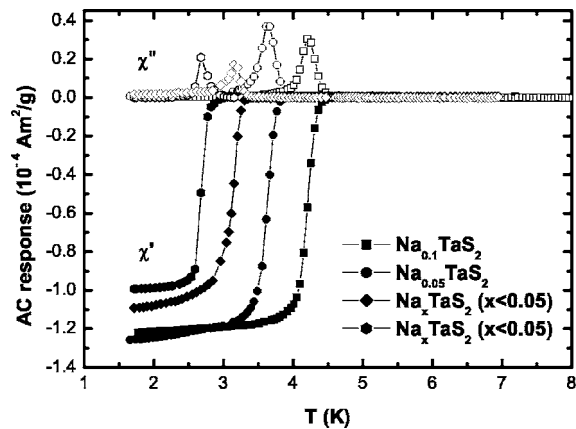
TABLE I. Sodium extent intercalated into $2H$-$TaS_2$ analyzed by the EDX of SEM.

| $T_c$ | at % (Na:Ta) | Formula |
|---|---|---|
| 4.4 K | 2.62: 27.09 | $Na_{0.1}TaS_2$ |
| 4.0 K | 1.22: 25.90 | $Na_{0.05}TaS_2$ |
| 3.4 K | sodium% <1 | $Na_xTaS_2$ ($0<x<0.05$) |
| 3.0 K | sodium% <1 | $Na_xTaS_2$ ($0<x<0.05$) |

### B. AC diamagnetism and EDX of SEM

It is found that both the $T_c$ and size of crystal are related to the cooling rate. Figure 4 shows four superconducting transition curves of four samples. The $T_c$ determined in the diamagnetic measurement changes from 4.4 K to 3.0 K, which is defined by the onset point of the real part of the AC susceptibility. The transition width of each curve is less than 0.5 K, which indicates a complete Meissner shielding effect. Because the biggest crystal has the highest $T_c$, it is natural to suppose that the increase of $T_c$ is related to the change of sodium content, which is controlled by the time and extent of diffusion. In order to know the sodium content, these crystals were analyzed with the EDX of SEM. Taking account of the possible inhomogeneity existing in the samples, we selected multiple points on each crystal surface and analyzed. The EDX spectrum showed that the atomic concentration of different analyzed regions were similar, which indicates that these crystals are homogeneous. Table I gives the sodium content of crystals analyzed by EDX of SEM. $T_c$ rises roughly with the increase of Na content in these crystals. As to the crystals with $T_c$ are equal to 3.4 K and 3.0 K, respectively, little sodium ions are detected by EDX. Because the $T_c$ of $2H$-$TaS_2$ is 0.8 K, thus, the sodium content in these two crystals are approximately between 0 and 0.05.

Figure 5 shows the EDX spectrum of the $Na_{0.05}TaS_2$ crystal. The characteristic peak of sodium around 1.1 keV is obvious. No signal of chlorine ions appear in the spectrum. The spectrum of the $Na_{0.1}TaS_2$ crystal is similar to that of the $Na_{0.05}TaS_2$ crystal, but the peak of sodium gets enhanced for the former.



FIG. 4. AC diamagnetism ($H_{AC}=1$ Oe, $f=333$ Hz) for a series of $Na_xTaS_2$ crystals. Analysis using EDX reveals that the sodium content is slightly different among the samples.
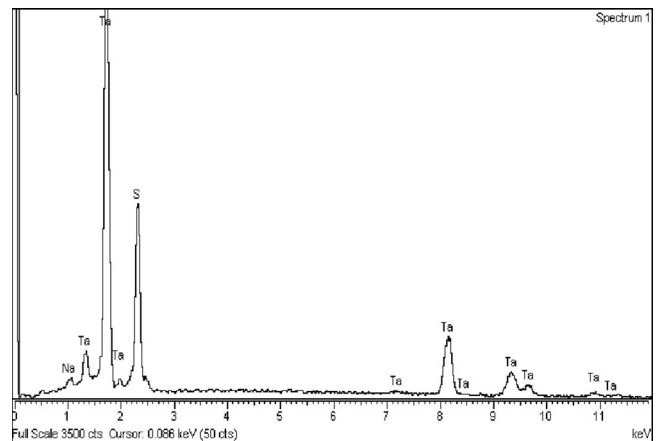


FIG. 5. EDX spectrum of the $Na_{0.05}TaS_2$ crystal. The characteristic peak of sodium around 1.1 keV is obvious.

It is generally believed that superconductivity in the dichalcogenides is due to electron-phonon coupling and is of the conventional BCS type. According to BCS theory, $T_c$ rises when the density of states at the Fermi surface is increased, which is inferred by the following formula:

$$T_c \propto \Theta_D \exp[-1/VN(E_F)], \qquad (1)$$

where $\Theta_D$ is the Debye temperature, $V$ is the electron-electron interaction which consists of the attractive electron-phonon-induced interaction subtracted by the repulsive Coulomb interaction, and $N(E_F)$ is the density of states at the Fermi surface. As to our knowledge, the change of $V$ was rarely reported when atoms or molecules are intercalated into TMDC's. Gample *et al.*[4] pointed out that the electron-phonon interaction is confined to the metallic disulfide layers and insensitive to the distance between $MX_2$ layers caused by intercalation. Thus, on the basis of little change of electron-phonon interaction, it is considered that $N(E_F)$ plays an important role for the increase of $T_c$ in $Na_xTaS_2$.

Calculations of DOS for the conduction band of $2H\text{-}TaS_2$ showed that $E_F$ lies approximately at the mid-point of the $d_{z^2}$ band of Ta, and the $d_{z^2}$ band is half-filled (occupied by one electron per formula unit) and the DOS has a peak at the Fermi level.[9,10] When sodium ions are intercalated between the layers of $2H\text{-}TaS_2$, charges are transferred from sodium to the $d_{z^2}$ band of Ta. The rigid-band model of intercalation suggests that the host band structure is unaltered upon intercalation, with $E_F$ increasing to reflect the transfer of charges from the intercalant. Consequently the DOS at Fermi surface should decrease. This is in contradiction to the observation that the $T_c$ increases instead of decreasing when the sodium atoms are intercalated. We will show below that the DOS at the Fermi level may increase because of the suppression to the CDW, rather due to the charge transfer.

### C. The anisotropy of the upper critical field

As to our knowledge, the upper critical field $H_{c2}(0)$ of $Na_xTaS_2$ was rarely reported. We studied $H_{c2}(0)$ of one piece crystal of $Na_{0.1}TaS_2$ with $T_c=4.3$ K through diamagnetic and transport measurement. Figure 6 presents the AC susceptibility under different magnetic fields. The transition curve moves regularly down to lower temperatures with increasing the magnetic field. Since the vortex motion is involved in the AC susceptibility measurement, it is difficult to define the onset point for superconductivity. Therefore in the following we will use resistive transport measurement to determine the upper critical field.

Figure 7 shows the in-plane resistance (*ab* plane) of the crystal $Na_{0.1}TaS_2$ at zero field. Decreasing temperature from 10 K to 4.9 K, the resistance $\rho$ changes subtly, and an abrupt superconducting transition happens at 4.83 K, zero resistance is obtained at about 4.3 K. A sharp transition with width less than 0.5 K indicates the good quality of the crystal $Na_{0.1}TaS_2$. The zero superconducting transition temperature is 4.3 K, which is consistent with the result of AC susceptibility.

In order to determine the upper critical field and the anisotropy of superconductivity, we measured the resistive
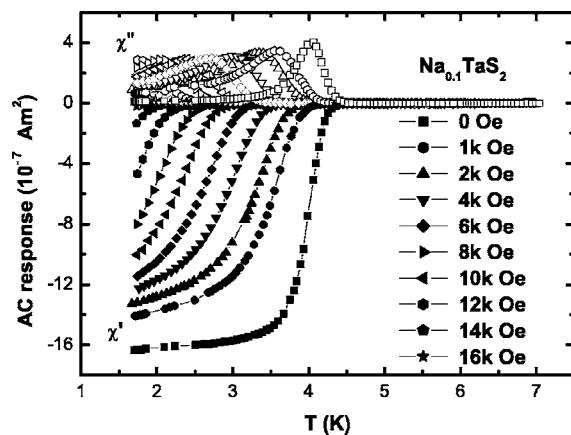


FIG. 6. AC susceptibility ($H_{AC}=1$ Oe, $f=333$ Hz) under different dc magnetic fields for the crystal $Na_{0.1}TaS_2$. Here the dc magnetic field is applied along the *c*-axis.

transitions at different magnetic fields with the field direction along the *ab*-plane [Fig. 8(a)] and *c*-axis [Fig. 8(b)]. One can see that the resistive curve shifts parallel down to lower temperatures with the increase of magnetic field. From the mid-point of the transition curves, we determine the upper critical fields for both directions which are shown in Fig. 9. In the Ginzburg-Landau theory, it is known that $H_{c2}=\Phi_0/2\pi\xi^2$ and $\xi\propto\sqrt{(1+t^2)/(1-t^2)}$, with $\Phi_0$ the flux quanta, $\xi$ the coherence length, $t=T/T_c$ the reduced temperature, thus one has

$$H_{c2}(T) = H_{c2}(0)\frac{1-t^2}{1+t^2}. \qquad (2)$$

We use the above equation to fit our data and show them as the solid and dashed lines in Fig. 9. The zero temperature upper critical fields $H_{c2}(0)$ determined in this way are $H_{c2}^{\|c}(0)=2.5T$ and $H_{c2}^{\|ab}(0)=16T$, therefore the anisotropy $H_{c2}^{\|ab}(0)/H_{c2}^{\|c}(0)=\xi_{ab}(0)/\xi_c(0)=\sqrt{m_c/m_{ab}}=6.4$, where $m_c$ and $m_{ab}$ are the effective mass tensors when the electrons are moving perpendicular and parallel to the $TaS_2$ layers. This
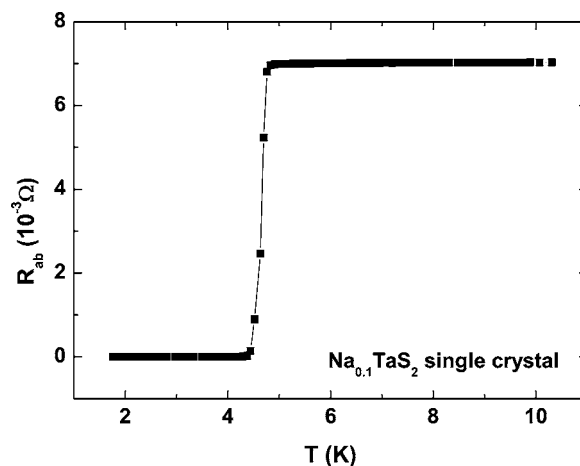


FIG. 7. In-plane resistance (*ab* plane) vs temperature for one piece of crystal $Na_{0.1}TaS_2$ under zero field. The transition width is less than 0.5 K.
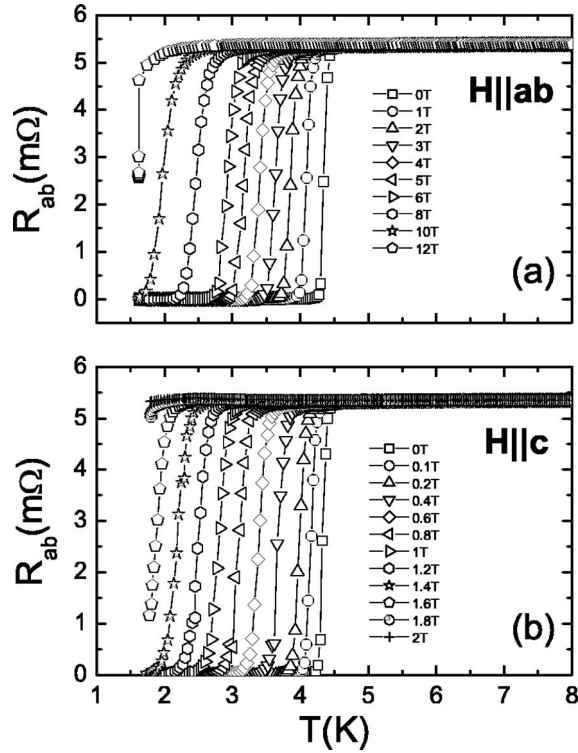
FIG. 8. The superconducting transition measured at different magnetic fields when the field is applied (a) perpendicular to and (b) parallel to the c-axis. From the midpoint of the resistive curve one can determine the upper critical field $H_{c2}(T)$.

value is quite close to that of optimally doped $YBa_2Cu_3O_7$. This is to our surprise since the sample here is clearly of thin-platelet shape which looks like the much more anisotropic curate system $Bi_2Sr_2CaCu_2O_8$ single crystals. Actually the zero temperature value of upper critical field can also be determined through the Werthamer-Helfand-Hohenberg (WHH) formula[24]

$$H_{c2}(0) = -0.693 T_c \left( \frac{dH_{c2}}{dT} \right)_{T=T_c}. \quad (3)$$
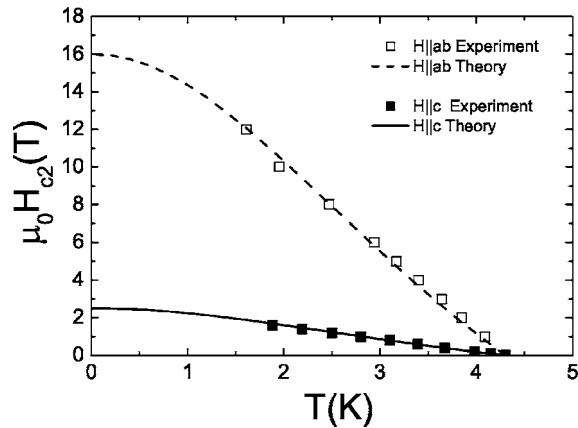


FIG. 9. The upper critical field determined from the midpoint of the transition curve. The solid and dashed lines here are theoretical curves of $H_{c2}(T) = H_{c2}(0)[(1-t^2)/(1+t^2)]$ with $H_{c2}^{\|c}(0) = 2.5T$ and $H_{c2}^{\|ab}(0) = 16T$.



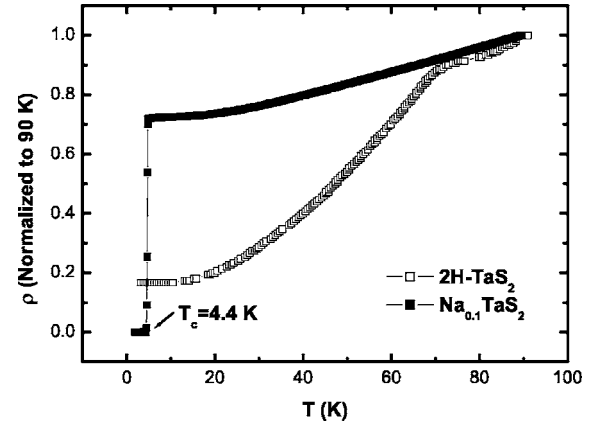FIG. 10. Comparison of resistivity between $2H\text{-}TaS_2$ and $Na_{0.1}TaS_2$. For clarity, here we show only the data from 2 K to 90 K. Resistivity of $2H\text{-}TaS_2$ is adopted from Ref. 11.

Here $dH_{c2}/dT$ is the slope of $H_{c2}(T)$ near $T_c$, which is about $0.7163\ T/K$ for $H\|c$ and $4.5\ T/K$ for $H\|ab$. Using above formula the zero temperature values of upper critical fields are $H_{c2}^{\|c}(0) = 2.13T$ and $H_{c2}^{\|ab}(0) = 13.4T$, which are close to the values determined in fitting the data to Eq. (2).

### D. Suppression to CDW by sodium intercalation

Trigonal prismatic layer compound $2H\text{-}TaS_2$ generally exhibits a charge-density-wave related phase transition accompanied by a drop in resistivity around 70 K.[12] It is thus interesting to measure the resistivity of our samples to high temperatures to see whether the CDW transition is still there. We thus measured the resistivity of crystals of $Na_{0.1}TaS_2$ from 2 K to 300 K. It is found that the resistivity $\rho$ decreases with the temperature smoothly and the superconducting transition happens at 4.4 K, no sudden drop of resistance on the resistivity curve was observed above $T_c$. Figure 10 shows the comparison of resistivity between undoped $2H\text{-}TaS_2$ and our sample $Na_{0.1}TaS_2$. From here it is tempting to conclude that the CDW is completely suppressed in our samples.

For further verification of the result obtained from $Na_{0.1}TaS_2$, we measured the resistivity of one crystal $Na_{0.05}TaS_2$ and show them in Fig. 11. The CDW-like drop in resistivity curve is also completely absent in the temperature region from 2 K to 300 K. This result provides convincing evidence that there is a competition between the superconductivity and charge density wave in layered chalcogenide $Na_xTaS_2$. When sodium ions are intercalated into $2H\text{-}TaS_2$, CDW order is destroyed and $T_c$ increases. The suppression to the CDW may be understood by the better c-axis conduction after the sodium intercalation. In this case the system deviates from two dimensionality as in $2H\text{-}TaS_2$ and thus prevents the lattice instability. This is partially supported by the relatively small anisotropy of $m_c/m_{ab}$ as determined above in the sodium intercalated samples. When the CDW is suppressed, the effective DOS at the Fermi surface is eventually enhanced leading to a much higher $T_c$.
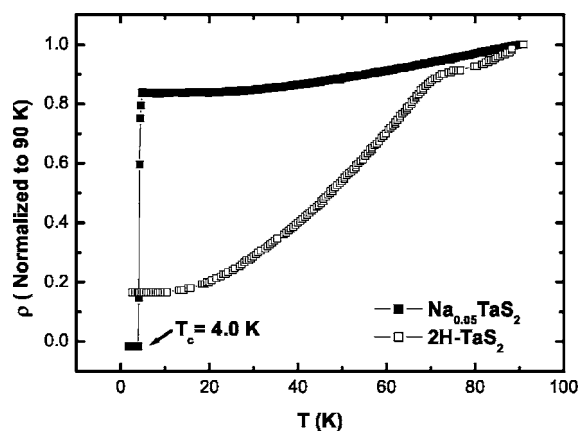
FIG. 11. Comparison of resistivity between $2H\text{-}TaS_2$ and $Na_{0.05}TaS_2$. For clarity we show here only the data from 2 K to 90 K. Resistivity of $2H\text{-}TaS_2$ is adopted from Ref. 11.

### E. Anisotropy of resistivity and the competition between superconductivity and CDW

In pyridine intercalated systems, the anisotropy of DC resistivity is in the order of $10^5$ along the $c$-axis and $ab$-plane. This extremely high anisotropy is far beyond the value we can expect in our present system. Therefore intercalating sodium here may enhance the electrical conduction along the $c$-axis and suppress the feature of two dimensionality. To check whether this is true, we measured the in-plane and off-plane resistivity for two samples, one with $x=0.10$ and $T_c=4.2$ K, and another with $x \leqslant 0.05$ and $T_c=2.5$ K (determined as the midpoint of the resistive transition). In Fig. 12, we present the temperature dependence of the (a) in-plane and (b) off-plane resistivity for the sample with $x=0.10$ and $T_c=4.2$ K. No trace of CDW can be observed here. Furthermore, one can easily see that the temperature dependence of the in-plane resistivity for this sample is rather linear in quite a wide temperature region. This result has been repeated in all our samples with $T_c$ higher than 4 K. This behavior resembles that of cuprate superconductors at optimal doping (with the highest $T_c$ in the same system). It remains an interesting question that whether this linear behavior observed here has any intact correlation with that in high-$T_c$ cuprate superconductors. We can also determine the anisotropy of resistivity for this sample at different temperatures. It is found that $\rho_c/\rho_{ab}$ is about 63.6 at 10 K and 5.3 at 300 K. Surprisingly the off-plane resistivity shows a clear semiconducting behavior indicating totally different electron conduction behavior when current is flowing along the plane or perpendicular to it. This interesting weak semiconducting behavior of $c$-axis resistivity has also been repeated in our samples with high $T_c$. Accompanying with this semiconducting behavior, a $c$-axis lattice modulation (with the modulation spacing of about $4c$) has been observed only in these samples with high $T_c$. Detailed analysis about the correlation with the resistive transport property, CDW and superconductivity is under way and will be published separately. For the less intercalated sample ($x \leqslant 0.05$ and $T_c=2.5$ K), the situation becomes very different. As shown in Figs. 13(a) and 13(b), one can see that a CDW transition occurs at about
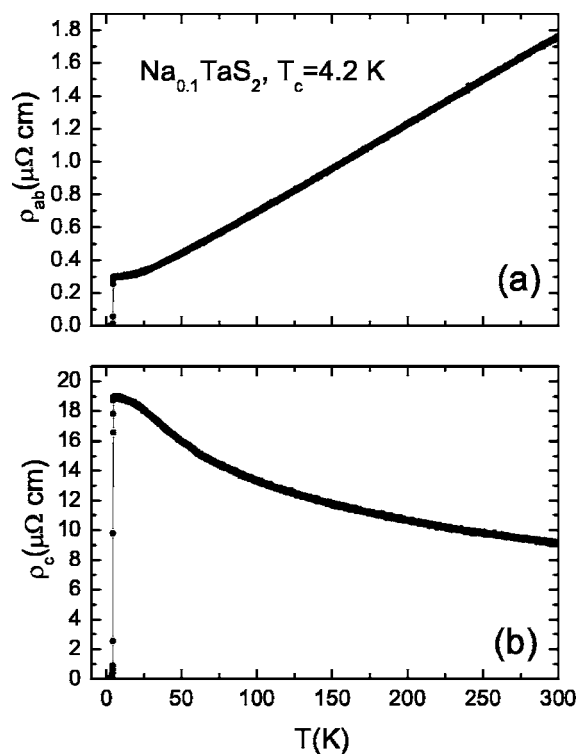


FIG. 12. Temperature dependence of (a) in-plane and (b) off-plane resistivity for the sample $Na_{0.1}TaS_2$. One can see that the in-plane resistivity shows a metallic behavior, but the off-plane one has an insulating behavior above $T_c$. The anisotropy of resistivity is about 63.6 at 10 K and 5.3 at 300 K. On both curves we cannot see any trace of CDW. A linear behavior of the in-plane resistivity is observed in wide temperature range. This resembles that in optimally doped high-$T_c$ cuprate superconductors.

65 K. Worthy of noting here is the much higher anisotropy of the resistivity. One can see that $\rho_c/\rho_{ab}$ is about 5000 at 10 K and 300 at 300 K. The anisotropy of resistivity in this less intercalated sample is about 60–100 times higher than that in the more intercalated sample ($x=0.1$, $T_c=4.2$ K) although a metallic behavior is observed above $T_{CDW}$ in these less intercalated samples. The much more higher anisotropy in these less intercalated samples may also interpret why the CDW appears in this sample. The strange metal-insulator (M-I) transition of the off-plane resistivity at $T_{CDW}$ in the present sample is a very interesting issue and the discussion on it may exceed the scope of this paper. It must be mentioned that this M-I transition can only be observed in relatively thick samples (above 0.2 mm). In rather thin samples, the $c$-axis resistivity shows the similar behavior of the in-plane resistivity without showing the M-I transition at the $T_{CDW}$. We attribute the disappearance of the M-I transition to the significant in-plane component of the total voltage drop on the two voltage leads attached to the two opposite surfaces if the leads are slightly asymmetric. Detailed analysis and discussion of the temperature dependence of resistivity for samples with systematic intercalated Na content will be presented in a forthcoming paper. We must point out that, since the thickness of the sample is very thin (typically in the scale of 0.1 mm to 0.2 mm), to precisely measure the off-plane resistivity is really a problem. Thus it may subject to correc-
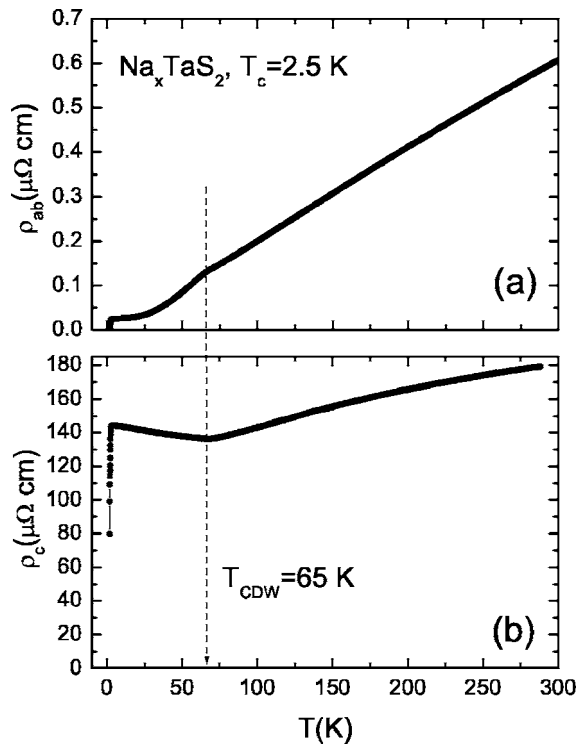
FIG. 13. Temperature dependence of (a) in-plane and (b) off-plane resistivity of a sample $Na_xTaS_2$ with $x \leq 0.05$ and $T_c = 2.5$ K. A clear kink corresponding to the CDW transition can be seen here. One can also see that the in-plane resistivity shows metallic behavior in wide region of temperature, but the off-plane resistivity first shows a metallic behavior above $T_{CDW}$ and an insulating behavior below $T_{CDW} = 65$ K. The anisotropy of resistivity is about 5000 at 10 K and 300 at 300 K.

tions in the future with more refined measurements. However the correction, if any in the future, will be within the range of about 20%, especially for the in-plane resistivity. In addition, we believe that the general temperature dependence of resistivity measured here will not be altered too much. Therefore the resistive data measured here may provide an useful platform for further understanding the interplay between CDW and superconductivity. Although we are not sure why the slight intercalation of Na can change the anisotropy and the electronic behavior so drastically, it may be safe to conclude that the higher anisotropy in the sample with less Na content enhances the 2D behavior and thus favors the structural instability leading to the CDW transition. This consequently suppresses the effective DOS at $E_F$ and lowers the superconducting transition temperature.

## IV. CONCLUSION

A new way to grow crystals of $Na_xTaS_2$ is presented. A series of crystals with different superconducting transition temperatures $T_c$ ranging from 2.5 K to 4.4 K were obtained. It is found that $T_c$ rises with the increase of Na content determined from the EDX of SEM. Compared with the resistivity curve of $2H$-$TaS_2$ ($T_c = 0.8$ K, $T_{CDW} \approx 70$ K), no signal of charge density wave (CDW) was observed in our present samples $Na_{0.1}TaS_2$ and $Na_{0.05}TaS_2$. The upper critical field and its anisotropy (about 6.4 for sample with $x = 0.1$ and $T_c = 4.2$ K) have also been determined. The anisotropy of resistivity is strongly suppressed together with the missing of the CDW in samples with higher $T_c$ and more Na content. In samples with less Na content and lower $T_c$, the CDW can be easily observed. It is concluded that there is a competition between the superconductivity and the CDW order: The rise of $T_c$ in $Na_xTaS_2$ by increasing the sodium content may be caused by the increase of DOS at Fermi surface when the CDW is suppressed.

*Electronic address: hhwen@aphy.iphy.ac.cn

[1] T. Valla, A. V. Fedorov, P. D. Johnson, J. Xue, K. E. Smith, and F. J. DiSalvo, Phys. Rev. Lett. **92**, 086401 (2004); **85**, 4759 (2000).

[2] J. A. Wilson and A. D. Yoffe, Adv. Phys. **28**, 193 (1969).

[3] A. H. Castro Neto, Phys. Rev. Lett. **86**, 4382 (2001).

[4] F. R. Gamble, J. H. Osiecki, M. Cais, and R. Pisharody, Science **174**, 493 (1971).

[5] F. Sernetz, A. Lerf, and R. Schöllhorn, Mater. Res. Bull. **9**, 1597 (1974).

[6] A. Lerf, F. Sernetz, W. Biberacher, and R. Schöllhorn, Mater. Res. Bull. **14**, 797 (1979).

[7] D. C. Johnston, Mater. Res. Bull. **17**, 13 (1982).

[8] H. P. Hughes and J. A. Scarfe, J. Phys.: Condens. Matter **8**, 1439 (1996).

[9] G. Y. Guo and W. Y. Liang, J. Phys. C **20**, 4315 (1987).

[10] K. Motizuki, N. Suzuki, and S. Tomishima, J. Magn. Magn. Mater. **104**, 681 (1992).

[11] P. Blaha, J. Phys.: Condens. Matter **3**, 9381 (1991).

[12] A. H. Thompson, F. R. Gamble, and R. F. Koehler, Phys. Rev. B **5**, 2811 (1972).

[13] H. E. Brauer, H. I. Starnberg, L. J. Holleboom, H. P. Hughes, and V. N. Strocov, J. Phys.: Condens. Matter **13**, 9879 (2001).

[14] H. I. Starnberg, H. E. Brauer, L. J. Holleboom, and H. P. Hughes, Phys. Rev. Lett. **70**, 3111 (1993).

[15] H. E. Brauer, H. I. Starnberg, L. J. Holleboom, V. N. Strocov, and H. P. Hughes, Phys. Rev. B **58**, 10031 (1998).

[16] C. Pettenkofer and W. Jaegermann, Phys. Rev. B **50**, 8816

(1994).

[17] L. F. Mattheiss, Phys. Rev. B **8**, 3719 (1973).

[18] A. Meetsma, G. A. Wiegers, R. J. Haange, and J. L. De Boer, Acta Crystallogr., Sect. C: Cryst. Struct. Commun. **C46**, 1598 (1990).

[19] A. H. Thompsom, Comments Solid State Phys. **7**, 125 (1976).

[20] A. Schlicht, M. Schwenker, W. Biberacher, and A. Lerf, J. Phys. Chem. B **105**, 4867 (2001).

[21] C. Pettenkofer, W. Jaegermann, A. Schellenberger, E. Holub-Krappe, C. A. Papageorgopoulos, M. Kamaretos, and A. Papageorgopoulos, Solid State Commun. **84**, 921 (1992).

[22] C. Dong, J. Appl. Crystallogr. **32**, 838 (1999).

[23] L. E. Conroy and K. R. Pisharody, J. Solid State Chem. **4**, 345 (1972).

[24] N. R. Werthamer, E. Helfand, and P. C. Hohenberg, Phys. Rev. **147**, 295 (1966).